Present Terrestrial Heat Flow Measurements of the Geothermal Fields in the Chagan Sag of the Yingen-Ejinaqi Basin, Inner Mongolia

FENG Renpeng[1, 2, 3], ZUO Yinhui[1, 2, 3, *], YANG Meihua[1, 2, 3], ZHANG Jiong[4], LIU Zhi[4], ZHOU Yongshui[5] and HAO Qingqing[6]

1. *State Key Laboratory of Oil and Gas Geology and Exploitation, Chengdu University of Technology, Chengdu 610059, China*
2. *Shandong Provincial Key Laboratory of Depositional Mineralization & Sedimentary Minerals,Shandong University of Science and Technology, Qingdao 266590, China*
3 *State Key Laboratory of Petroleum Resources and Prospecting, China University of Petroleum, Beijing 102249, China*
4 *Geothermal and Environmental Research Institute, Institute for Global Environment Change, Xi'an Jiaotong University, Xi'an 710049, China*
5 *Research Institute of Exploration and Development, Zhongyuan Oilfield, SINOPEC, Puyang 457001, China*
6 *Institute of Mineral Resources Research, China Metallurgical Geology Bureau, Beijing 100025, China*

Abstract: Owing to the lack of terrestrial heat flow data, studying lithospheric thermal structure and geodynamics of the Yingen-Ejinaqi Basin in Inner Mongolia is limited. In this paper, the terrestrial heat flow of the Chagan sag in the Yingen-Ejinaqi Basin were calculated by 193 system steady-state temperature measurements of 4 wells, and newly measuring 62 rock thermal conductivity and 20 heat production rate data on basis of the original 107 rock thermal conductivity and 70 heat production data. The results show that the average thermal conductivity and heat production rate are 2.11 ± 0.28 W/(m·K) and 2.42 ± 0.25 μW/m^3 in the Lower Cretaceous of the Chagan sag. The average geothermal gradient from the Lower Suhongtu 2 Formation to the Suhongtu 1 Formation is 37.6 °C/km, and that of the Bayingebi 2 Formation is 27.4 °C/km. Meanwhile, the average terrestrial heat flow in the Chagan sag is 70.6 mW/m^2. On the above results, it is clear that there is an obvious negative correlation between the thermal conductivity of the stratum and its geothermal gradient. Moreover, it reveals that there is a geothermal state between tectonically stable and active areas. This work may provide geothermal parameters for further research of lithospheric thermal structure and geodynamics in the Chagan sag.

Key words: thermophysical parameters, geothermal gradient, terrestrial heat flow, Chagan sag, Yingen-Ejinaqi Basin

Corresponding Author: Zuo Yinhui, Email: zuoyinhui@tom.com.
First Author: Feng Renpeng, Email: fengrpeng@163.com.

1 Introduction

Terrestrial heat flow is the most direct result of Earth's internal heat on the surface. It reflects the lithospheric thermal state and energy balance and can provide rich geological, geophysical, and geodynamic information (Furlong and Chapman, 1987; Pollack et al., 1993). Since the first measurement of continental terrestrial heat flow in 1939, it has been the focus of many international studies (Chapman, 1984; Ranalli and Rybach, 2005; Duchkov et al., 2010; Hasterok et al., 2011; Kukkonen et al., 2011; Leszek and Konrad, 2012; Zou Yinhui., 2011, 2014, 2017a; Carson et al., 2014; Ruepke et al., 2017). However, the study of the terrestrial heat flow in China began relatively late. Since 1966, three heat flow data for the Mesozoic basin in Northeast China have been reported (Yi Shanfeng, 1966), but terrestrial

This article has been accepted for publication and undergone full peer review but has not been through the copyediting, typesetting, pagination and proofreading process, which may lead to differences between this version and the Version of Record. Please cite this article as doi: 10.1111/1755-6724.13761.

heat flow values were not officially released until 1979 (The geothermal research group of the Institute of Geology, Chinese Academy of Sciences, 1979). As of 2016, 1,230 measurements of terrestrial heat flow have been published (Jiang Guangzheng et al., 2016). However, these data are mainly for the Tarim Basin, the Sichuan Basin, the Bohai Bay Basin, and the areas adjacent to these basins (Qiu Nansheng, 2001, 2003; Wang Liangshu et al., 2002; Gong Yulin et al., 2003; Wang Yongxin and Feng Diansheng, 2003; Lu Qingzhi et al., 2005; Feng Changge et al., 2009; Xu Ming et al., 2011; Zuo Yinhui et al., 2011, 2015a, 2017a; Li Zongxing et al., 2015; Liu Shaowen et al., 2015; Chang Jian et al., 2016; Chen Aihua et al., 2017; Liu Qianqian et al., 2017; Zhou Yang et al., 2017). Meanwhile, there are only nine estimated terrestrial heat flow data available for the Yingen-Ejinaqi Basin in Inner Mongolia (Zuo Yinhui et al., 2013b, 2015a).

The Yingen-Ejinaqi Basin is a medium-large basin in China that has yet to be explored extensively for oil and gas sources. The Chagan sag in the Yingen-Ejinaqi Basin has the most exploration prospects (Zuo Yinhui et al., 2013a; Wang Shenglang et al., 2016). At present, the Chagan sag has more than 100 wells, which will facilitate the measurements of the system steady-state temperature, rock thermal conductivity and heat generation rate. In 2016, a joint team of researchers from Xi'an Jiaotong University, Chengdu University of Technology, the Institute of Geology and Geophysics, Chinese Academy of Sciences, and the Zhongyuan Oilfield conducted system steady-state temperature measurements in four typical wells in the Chagan sag. Based on the original 107 rock thermal conductivity and 70 heat production rate data (Zuo Yinhui et al., 2013a, 2015a), 62 rock thermal conductivity and 20 heat production rate were measured. Using these data, the geothermal gradient and terrestrial heat flow in the Chagan sag were calculated. Moreover, we investigated the factors influencing the geothermal gradient and the tectonic evolution of the terrestrial heat flow. The geothermal information obtained in this investigation is expected to be useful in evaluating the geothermal resources in the Chagan sag.

2 Geological Setting

2.1 Geological setting of the Yingen-Ejinaqi basin

The Yingen-Ejinaqi Basin is a Mesozoic rift basin that is developed on the base of the Precambrian crystalline block and the Paleozoic fold (Fig. 1) (Wang Chunyan et al., 2006). This basin is bounded by Lang Hill to the east, the Beida Hill and Yabulai Hill to the south, the North Hill to the west, and the China–Mongolia border, Honggeerji Hill, and Mengenwula Hill in the north. The Yingen-Ejinaqi Basin is located from 39° N to the Mongolian border and between 99°E and 108°E. The basin is about 600 km long and 75–255 km wide and has an area of about 12.3×10^4 km^2. The sedimentary rocks in the Mesozoic and Cenozoic is distributed over an area of 10.4×10^4 km^2 and consists of eight depressions and five uplifts.

Since the Triassic period, the Yingen-Ejinaqi Basin has experienced multiple stages of tectonic movement (Wei Pingsheng et al., 2005; Chen Qilin et al., 2006; Liu Xi et al., 2017; Wang Tianyang et al., 2017; Peng Heng et al., 2018; Chen Zhipeng et al., 2018). The basin mainly experienced four tectonic evolutions. (1) An initial rifting phase occurred during the Late Triassic to Jurassic. Due to the cessation of the Indochina plate movement, the basin entered a stage of uplifting and denudation during the late portion of the Late Triassic period. During the Early Jurassic, the basin entered a rifting stage because of the subduction of the Eastern Pacific plate and the southward movement of the Siberian plate. In the Middle Jurassic period, the rift in the study area was enhanced by the Yanshan II movement. In the Late Jurassic period, the Yanshan III movement caused the basin to enter another stage of uplifting and denudation. (2) An intense rifting phase occurred during the Early Cretaceous period. During this phase, significant rifting occurred in the basin largely owing to the Altun Fault and branch faults accompanied by a powerful volcanic eruption. (3) A depression phase occurred during the Late Cretaceous period. This phase was mainly influenced by the Yanshan IV movement, and the overall depression began giving rise to the basin that is present today. (4) Finally, an uplift phase occurred in the Cenozoic period. In this phase, the Yingen-Ejinaqi Basin was fully formed by an extrusion uplift due to the northward subduction of the Indian plate and the collision with the Eurasian plate. Of these stages, the tectonic movements at the end of the Late Jurassic and Early Cretaceous periods most significantly impacted the evolution of the basin.

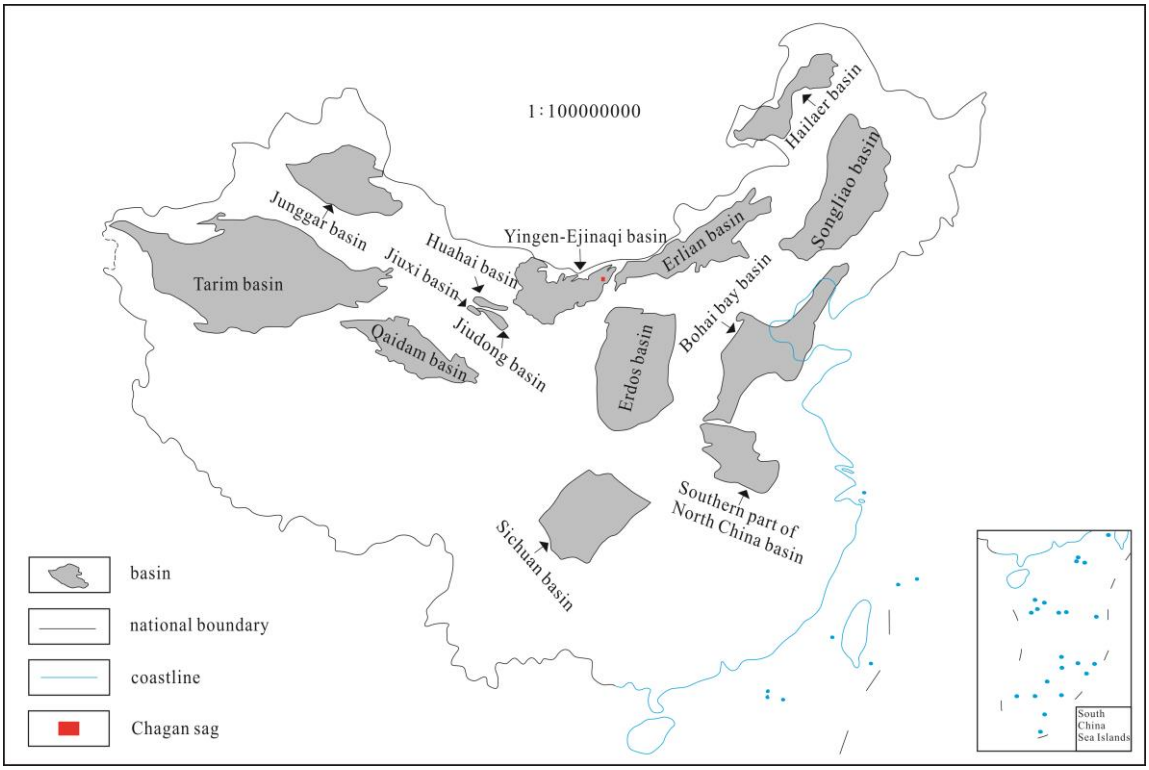

Fig. 1 Major oil and gas basins on land in China
(China basemap after China National Bureau of Surveying and Mapping Geographical Information)

2.2 Geological setting of the Chagan sag

The Chagan sag has the most oil and gas exploration prospects in the Yingen-Ejinaqi Basin. It is based on the ancient orogenic belt in the northwestern margin of the North China plate (Wang Xinwen and Tao Guoqing, 2008). The Chagan sag is located in the middle of the Chagandelesu Depression and is in the eastern margin of the Yingen-Ejinaqi Basin (Fig. 2). It is separated from the Baiyun sag by the Chugan uplift in the east and is bordered by the Lang Hill orogenic zone to the southeast, the Mubatu uplift to the southwest, the Xi'ni uplift to the west, and the Chulu uplift to the north. The Chagan sag is shaped like an irregular diamond, with an area of approximately 2,000 km^2, and is approximately 60 km long and 34 km wide. This sag has the thickest sedimentary layer and the most complicated tectonic evolution in the eastern Yingen-Ejinaqi Basin. The sag investigated herein comprises the northeast-to-southwest strike of the Chugan sag.

The Chagan sag is a typical half-graben rift basin developed on the Late Paleozoic fold base with a fault depression in the southwest and an overlying portion in the northeast. The stratum is thick in the west and thin in the east (Zuo Yinhui et al., 2015b; Wang Shenglang et al., 2016; Zuo Yinhui et al., 2017b). The multiple tectonic stresses in the Chagan sag result in a complex and diverse tectonic background and frequent tectonic activity. A well-developed fault lies mainly in the northeast-to-southwest direction. The current sag can be divided into three parts (from east to west): the Eastern subsag (including the Hailisu thrust zone, the Wuhua monoclinic zone, and the Hantamiao subsag zone), the Maodun uplift (including the central uplift zone), and the western subsag (including the wuliji fault-nose structural zone, the Ehen subsag, the central structural belt, and the Hule subsag).

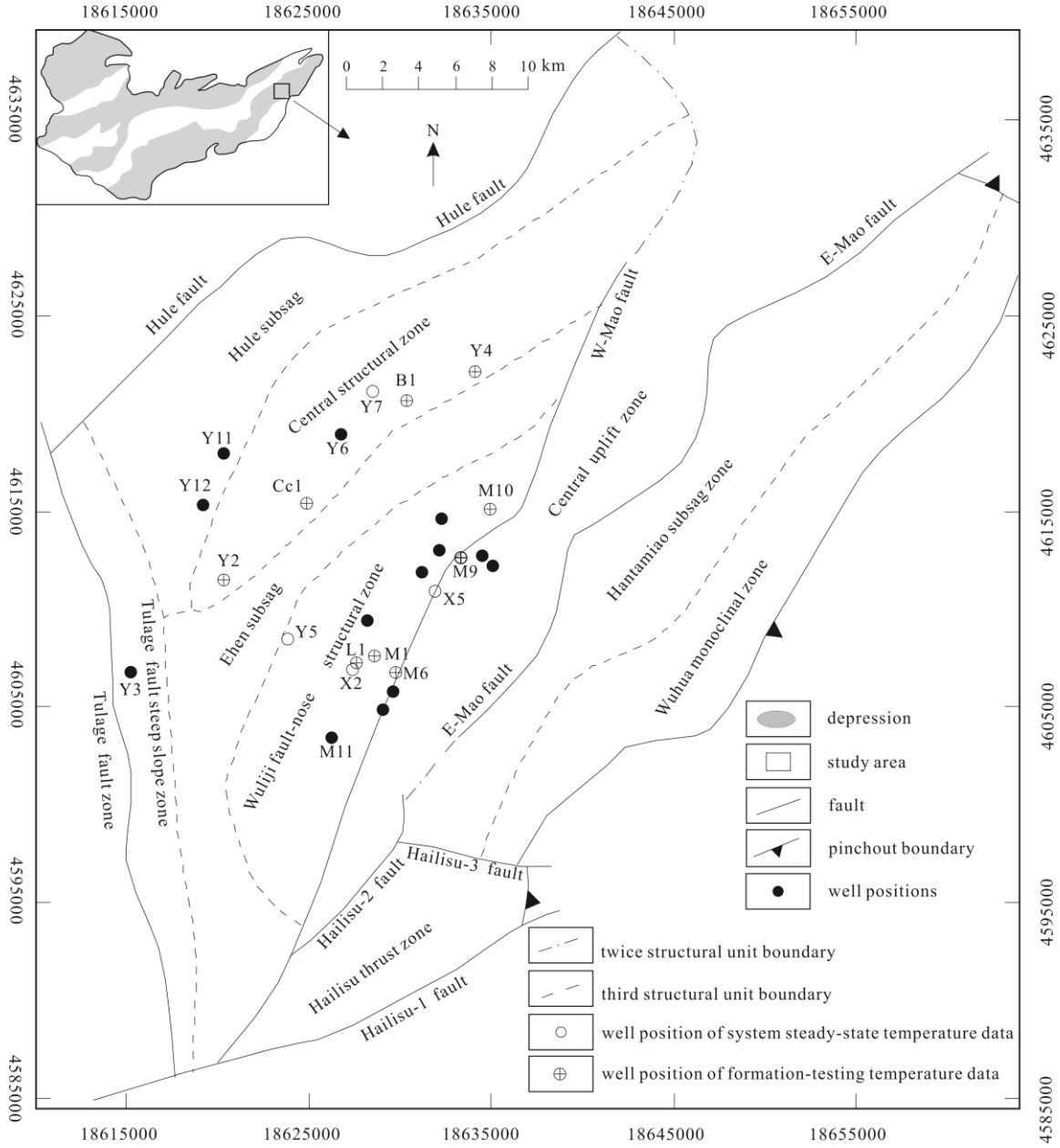

Fig. 2 Structural unit division and well of the Chagan sag

The strata of the Chagan sag include (from bottom to top) the Bayingebi Formation in the Early Cretaceous epoch (including the Bayingebi 1 Formation and Bayingebi 2 Formation), the Suhongtu Formation (including the Suhongtu 1 Formation and Suhongtu 2 Formation), the Yingen Formation, and the Wulansuhai Formation in the Late Cretaceous and Cenozoic epochs (Fig. 3). Since the Cretaceous period, the Chagan sag has experienced four tectonic stages of evolution (Yang Guochen et al., 2013). The Chagan sag initially had a half-graben rifting structure with a fault depression in the southwest and an overlying portion in the northeast extending from the Bayingebi Formation to the Suhongtu Formation. (1) During the rifting phase, the early tectonic framework of the Chagan sag was formed. As the volcanic activity was strong, the intrusion of volcanic rocks formed the Maodun subbulge (i.e., the central uplift zone) in the middle of the sag. (2) Next, in the faulted depression phase in the Early Cretaceous period, the Yingen Formation was deposited, the faults were weakened, and the volcanic activity decreased. (3) During the ensuing depression stage in the Late Cretaceous period, the Wulansuhai Formation was deposited, the plate was stretched, the entire depression sank, the fracturing ceased, and the volcano was

dormant. (4) Finally, in the uplifting phase in the Cenozoic period, an extrusion uplift and thrust occurred in the sag. In the southwestern part of the sag, an extrusion structure belt (i.e., the Hailisu thrust zone) was formed between two thrust-fault zones.

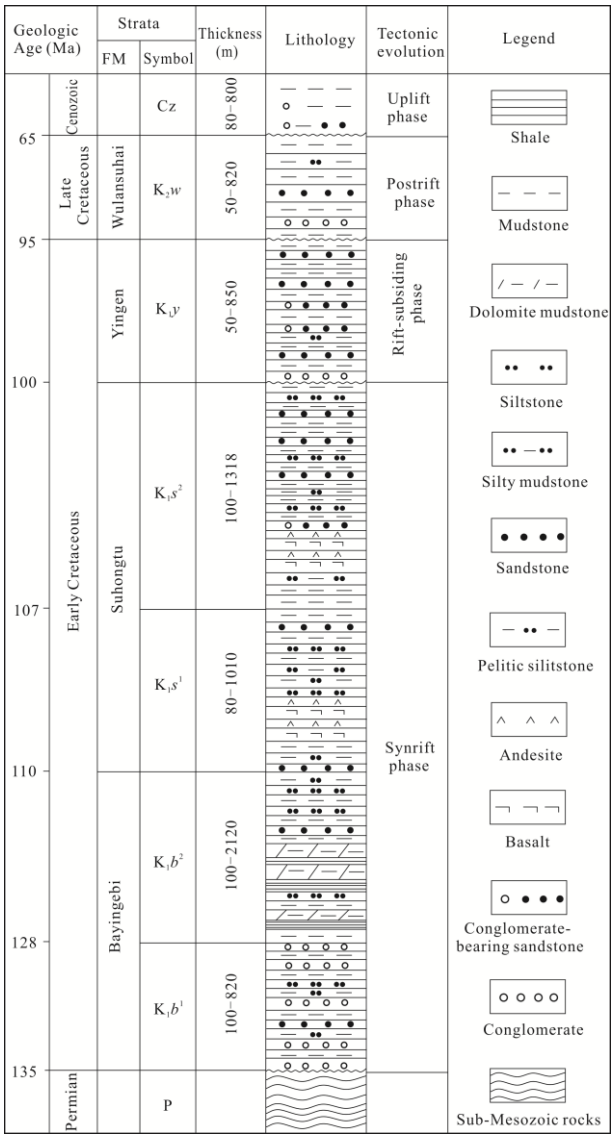

Fig. 3 Stratigraphic column section of the Chagan sag

FM = Formatiom

3 Methods and Parameters

3.1 Methods

3.1.1 Calculation of terrestrial heat flow

Terrestrial heat flow is a comprehensive parameter reflecting the characteristics of a geothermal field. Under one-dimensional steady-state heat-conduction conditions, terrestrial heat flow, q (mW/m^2), can be obtained as the product of the vertical geothermal gradient, G (°C/km), and the thermal conductivity of the rock, K (W/(m·K)) (Eq. 1) (The geothermal research group of the Institute of Geology, Chinese Academy of Sciences, 1979):

$$q = -K \times G. \quad (1)$$

A negative G or K value indicates the heat flow from the interior of the Earth to the surface.

3.1.2 Calculation of geothermal gradient

The value of G can be calculated as follows(Eq. 2) (Fig. 4):

$$G = (T_2 - T_1)/(Z_2 - Z_1), \quad (2)$$

where T_1 and T_2 are the temperatures (°C) at the top and bottom of the condensed section, respectively, and Z_1 and Z_2 are the depths (km) of the top and bottom of the stratum, respectively.

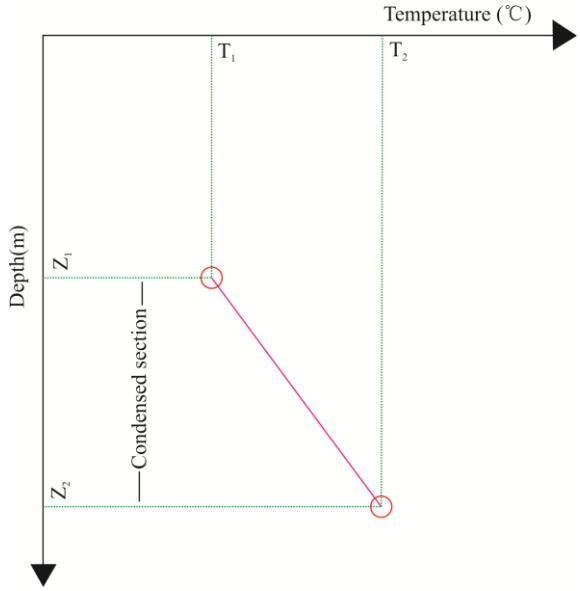

Fig. 4 Calculation model of geothermal gradient
G = Geothermal gradient;
T_1, T_2 are temperatures of the compacted section corresponding to burial depths Z_1, Z_2 for the same stratum.

3.2 Basic parameters

3.2.1 System Steady-State Temperature Data

At present, a total of 193 system steady-state temperature data of Wells X2, X5, Y5 and Y7 were tested and obtained (Tables 1–4). The Wells X2, X5 and Y5 are located in the Wuliji fault-nose structural zone, and the Well Y7 is located in the central structural zone. The formation temperature was measured from the Bayingebi 2 Formation to the Cenozoic epoch in Wells X2, X5, and Y7 and from the Cenozoic epoch to the Suhongtu Formation in Well Y5. Since the Cenozoic epoch is affected by factors such as solar radiation and groundwater disturbance, the formation temperatures of the Cenozoic epoch were not considered in the calculations.

3.2.2 Geothermal gradient

The Upper Cretaceous and Cenozoic epochs in the Chagan sag are not targeted layers for oil and gas exploration, so no core samples are available. The lithology is mainly mudstone, sandstone, and volcanic rock. In previous studies (Zuo et al., 2013b), the thermal conductivities of 62 rock samples from Wells Y7, Y5, and X5 were tested (Table 5). Here, the thermal conductivities of 169 rocks samples were measured at the Geothermal and Environmental Research Institute of Xi'an Jiaotong University.

3.2.3 Heat production rate

There were 90 heat production rate data in the Chagan sag, including existing 70 data (Zuo et al., 2015) and 20 newly measured data from samples of the Yingen Formation, the Suhongtu Formation, and the Bayingebi Formation taken at the Analytical Laboratory of Beijing Research Institute of Uranium Geology (Table 6). In these formations, the lithology is mainly mudstone, sandstone, and volcanic rock.

4 Results

4.1 Geothermal gradient

Figure 5 shows the relationship between the system steady-state temperature measurements and the recorded depths in Wells X2, X5, and Y7 (divided into three sections according to the depth) and Well Y5 (divided into two sections). The geothermal gradient was calculated using Eq. (1) on the basis of the steady-state system temperature data from the four wells (Table 7). The data from Well Y7 show that, in the Wuliji fault-nose structural zone, the geothermal gradient from the Wulansuhai Formation to the upper part of the Suhongtu 2 Formation was 27.3 °C/km, whereas that through the bulge area was 33.6 °C/km. The data from Wells X2, X5, and Y7 show that the geothermal gradient from the lower part of the Suhongtu 2 Formation to the Suhongtu 1 Formation was 37.6°C/km and that through the Bayingebi 2 Formation was 27.4 °C/km.

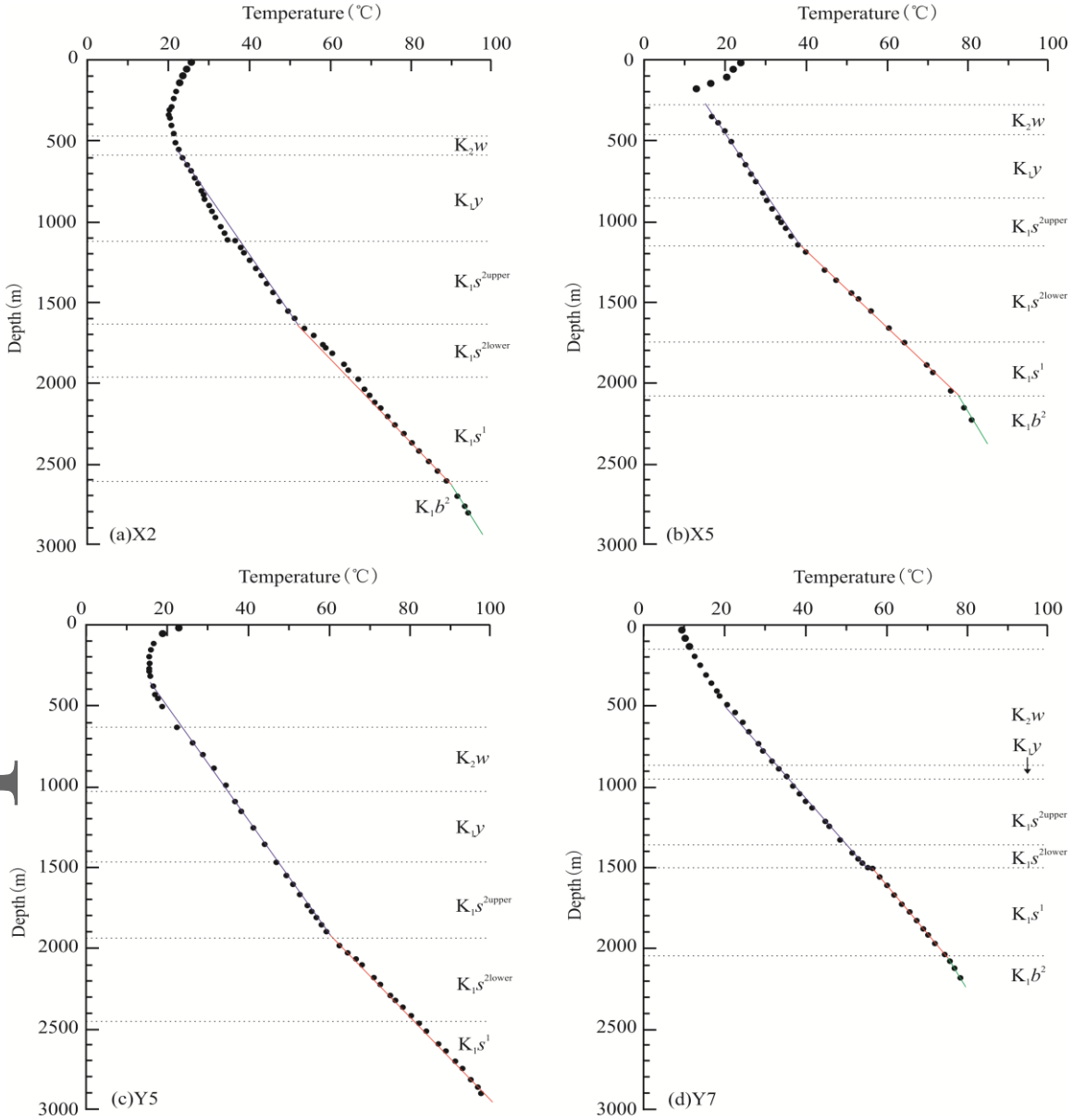

Fig. 5 System steady-state temperature data versus depth of 4 wells in the Chagan sag

4.2 Rock thermal conductivity

The results show that the thermal conductivity of the rock found in the Chagan sag ranges from 1.5 to 3.0 W/(m·K) (Fig. 6), increasing at greater depths. Considering only the lithology, the thermal conductivity of sandstone and magmatic rock increases with depth, but the change in the thermal conductivity of

mudstone is not obvious (Fig. 7). The strata are mainly the clastic rocks of the Suhongtu 1 Formation and the Bayingebi 2 Formation

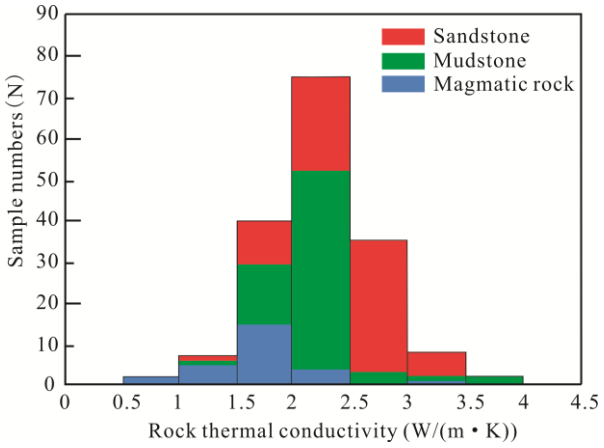

Fig. 6 Frequency distribution histogram of rock thermal conductivity in the Chagan sag

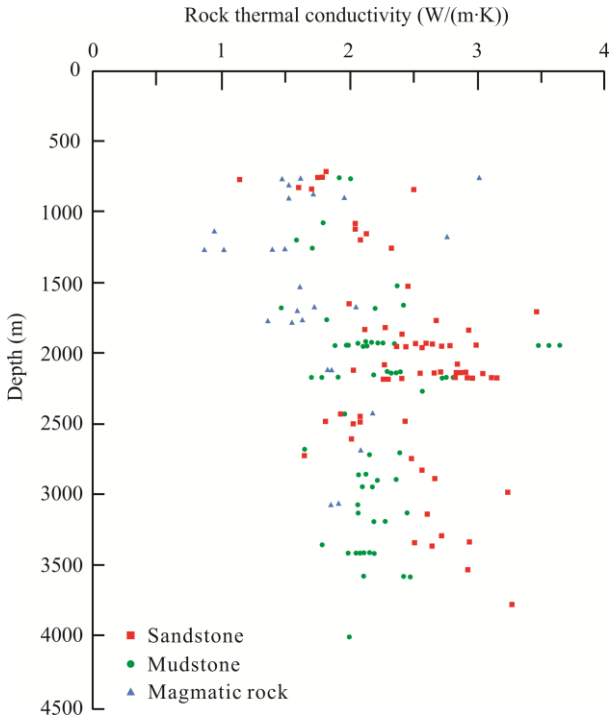

Fig. 7 Rock thermal conductivity data versus depth in the Chagan sag

According to the percentage of sandstone, mudstone, and magmatic rock in 21 wells, the thermal conductivities of the various strata were obtained as follows (Eq. 3) (Table 8):

$$K = K_s P_s + K_n P_n + K_m P_m, \quad (3)$$

where K_s, K_n, and K_m are the thermal conductivities of sandstone, mudstone, and magmatic rock (in W/(m·K)), respectively, and P_s, P_n, and P_m are the percentages of sandstone, mudstone, and magmatic rock, respectively. The average thermal conductivity was calculated as 2.11±0.28 W/(m·K).

4.3 Rock heat-generation rate

The average heat-generation rate in the rock of the Chagan sag was the largest in mudstone, followed by sandstone, and magmatic rock exhibited the lowest heat-generation rate (Fig. 8). This is because mudstone contains a large amount of radioactive material that can produce heat upon decay, whereas magmatic rocks

are relatively dense and have little radioactive material.

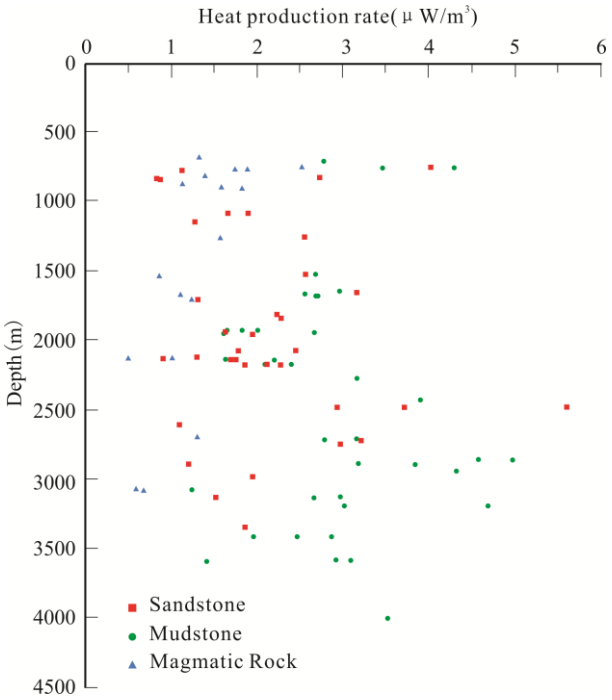

Fig. 8 Heat production rate data versus depth in the Chagan sag

According to the percentages of sandstone, mudstone, and magmatic rock in 21 wells, the heat-generation rates of various strata were obtained as follows (Eq. 4) (Table 9):

$$A = A_s P_s + A_n P_n + A_m P_m, \quad (4)$$

where A_s, A_n, and A_m are the heat-generation rates of sandstone, mudstone, and magmatic rock (in W/(m·K)), respectively., which were 2.12±0.98, 2.87±0.92, and 1.32±0.54 μW/m^3, respectively, in the Chagun sag. Thus, based on the lithology, the average heat-generation rate of the Lower Cretaceous epoch was 2.42±0.25 μW/m^3. This relatively high heat-generation rate reveals that the Chagan sag has higher energy and a higher geothermal gradient (Table 10) (Qiu Nansheng, 2001, 2002; Qiu, 2003; Feng et al., 2009; Rao Song et al., 2013; Liu et al., 2015; Li et al., 2015).

4.4 Terrestrial heat flow

Based on the thermal conductivity of the rock and the geothermal gradient, the terrestrial heat flow in each of the four wells was calculated using the thermal-resistance method (Chapman, 1984) (Table 11). The terrestrial heat flow in the Euliji fault-nose structure zone ranged from 61.0 to 81.0 W/m^2, averaging 70.9 W/m^2. The central tectonic belt had a terrestrial heat flow ranging from 65.1 to 69.1 W/m^2, averaging 67.5 W/m^2. Thus, the terrestrial heat flow in the Chagan sag is 70.6 mW/m^2, which is higher than the average continental terrestrial heat flow of 63 mW/m^2, indicating that the area has a high geothermal background (Hao Chunyan et al., 2014).

5 Discussions

5.1 Factors influencing the geothermal gradient and terrestrial heat flow

Sedimentary basins are usually stable geothermal systems. Thus, at a single drilling site, the terrestrial heat flow in different strata should be the same, and thus the strata with lower rock thermal conductivities should have higher geothermal gradients than those with higher rock thermal conductivities. Taking Well X5 as an example, the geothermal gradient curve can be divided into three sections (Fig. 9). (1) From the lower part of the Suhongtu 2 Formation to the Suhongtu 1 Formation, the lithology is mainly magmatic

rock in the lower parts of the Suhongtu 2 Formation and the Suhongtu 1 Formation and mudstone in the upper part of the Suhongtu 1 Formation. The thermal conductivity of the rock is low, around 1.98 W/(m·K), and the geothermal gradient is 40.9 °C/km. The W-Mao Fault may accelerate the heat loss from the shallow layers, which may increase the calculated terrestrial heat flow, but the effect should be small for the Chagan sag. (2) In the Bayingebi 2 Formation, the lithology is mainly sandstone and mudstone. The rock thermal conductivity is 2.33 W/(m·K) and the geothermal gradient is 26.2 °C/km. (3) From the Wulansuhai Formation to the upper part of the Suhongtu 2 Formation, the lithology is, again, mainly sandstone and mudstone. However, unlike in section (2), the thermal conductivity is 1.88 W/(m·K) and the geothermal gradient is 25.8°C/km.The results may be affected by the activity of the groundwater in addition to the rock thermal conductivity. Well Y7 is located in the bulge area of the central structural belt, and there are few faults in this area, but the structure is relatively stable and there is no groundwater findings indicate that the thermal conductivity of the rock has a significant influence on the geothermal gradient in this well. The geothermal gradient from the lower part of the Suhongtu 2 Formation to the Suhongtu 1 Formation is similar to that from the Wulansuhai Formation to the upper part of the Suhongtu 2 Formation, whereas that in the Bayingebi 2 Formation is smaller. Therefore, the geothermal gradient and rock thermal conductivity from the lower part of the Suhongtu 2 Formation to the Suhongtu 1 Formation and the Bayingebi 2 Formation were used to calculate the terrestrial heat flow in the Chagan sag.

The terrestrial heat flow in the Chagan sag was calculated from the system steady-state temperature data for the four wells as 70.6 mW/m^2. This result is slightly smaller than that estimated using measured oil temperature data (Zuo et al., 2013b). Moreover, this terrestrial heat flow is higher than those in structurally stable zones such as the Junggar Basin (43.2 mW/m^2) (Raisong et al., 2013), the Qaidam Basin (55.1 W/m^2) (Li Zongxing et al., 2015), the Baltic Shield (35–40 mW/m^2) (Čermák et al., 1993), and the Proterozoic craton (averaging 55.0±17 mW/m^2) (Rudnick et al., 1998). The terrestrial heat flow in the Chagan sag is lower than those in modern continental rifts, such as the Rhine Graben (85.0 mW/m^2) (Lysak, 1987), modern continental marginal expansion basins, such as the Yinggehai Basin (84 mW/m^2) (He Lijuan et al., 1998), and Cenozoic tectonic activity zones such as the American Cenozoic tectonic activity zone (83 mW/m^2) (Morgan, 1982). Therefore, the Chagan sag has a geothermal state between between tectonically stable and active areas.

5.2 Influence of tectonic evolution on terrestrial heat flow

The Mohorovičić discontinuity of the Yingen-Ejinaqi Basin is 41.5 km deep (Meng Lingshun et al., 1995), which is shallower than those in the Tarim Basin and the Qaidam Basin in the west, but deeper than those in the North China Basin and the Liaohe Basin in the east (Qiu Nansheng, 1998). However, the terrestrial flow in the Yingen-Ejinaqi Basin is larger than in these basins. This is because the Yingen-Ejinaqi Basin in the Chagan sag was formed by an extension of the Altun Fault in the northeast direction in the Early Cretaceous period and the strike-slip fault cut into the upper mantle of the lithosphere (Che Zicheng et al., 1998; Xu Zhiqing et al., 1999). This series of movements in combination with magma spurting and large tensile stresses and lithosphere thinning during the formation of the basin caused the mantle material to surge and brought in a significant amount of heat. The Early Cretaceous period exhibited the highest geothermal background. Today, the heat flow on the surface shows the persistence of this thermal state, but the heat flow is declining.

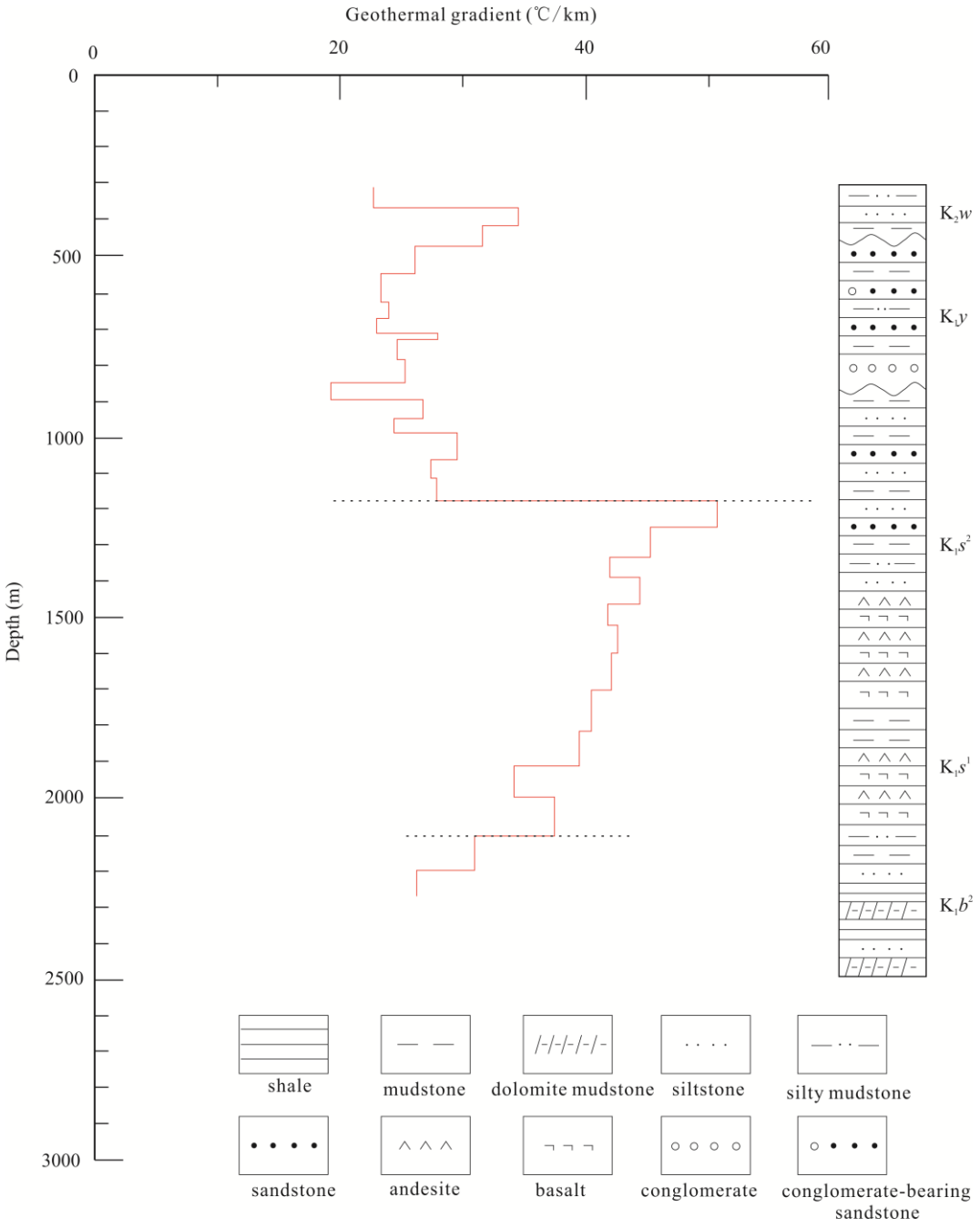

Fig. 9 Geothermal gradient of Well X5 versus depth in the Chagan sag

The basement of the Yingen-Ejinaqi Basin is an island-arc fold belt formed at the intersection of the North China plate, the Tarim Plate, and the Kazakhstan Plate during the Paleozoic period; it has the properties of a Paleozoic orogenic belt (Wu Tairan and He Guoqi, 1993). The Mesozoic and Cenozoic basins developed in this orogenic belt and between the deep faults of the Paleo-subduction zones and the Paleo-suture zones in a very complicated manner. Since the Paleogene period, the northward subduction of the Indian plate has caused it to collide with the Eurasian plate, and the Indian plate is still moving toward the Eurasian plate at a very slow speed. The Yingen-Ejinaqi Basin has been continuously squeezed by the collision between these two plates, causing the southwestern boundary of the basin to migrate northwards; this process continues to date (Yang Jinlin, 2011). In the meantime, the southeastern part of the basin is being subjected to the subduction of the Pacific plate in the WNW direction, causing the southeast boundary of the basin to migrate northwards. At the same time, the Siberian plate is blocking the northward movement of the Yingen-Ejinaqi Basin (Chen Changchun, 1994). Due to this complex situation,

the basin remains in a relatively high-temperature state today. Some reverse faults and folds have been found in the Shangdan Depression and the Chagandulesu Depression, but the tectonic movement in these areas is not as intense as in the modern continental marginal expansion basin and the Cenozoic tectonic activity zone. Together, these findings imply that the Yingen-Ejinaqi Basin is currently in a tectonic setting between tectonically active and structurally stable; this theory is consistent with the geothermal state revealed by the geothermal flow in the Chagan sag.

6 Conclusions

(1) In this study, we measured the heat production rates of the mudstone, sandstone, and magmatic rock in the Chagan sag as 2.87±0.92, 2.12±0.98, and 1.32±0.54 μW/m^3, respectively. Moreover, the average heat production rate of the Lower Cretaceous epoch in the Chagan sag was 2.42±0.25 μW/m^3. This relatively high heat-generation rate reveals that the Chagan sag has a higher energy and a more significant geothermal gradient;

(2) The rock thermal conductivity in the Chagan sag was measured to be 2.11±0.28 W/(m·K). Finally, we determined the average geothermal gradient of strata from the Suhongtu 2 Formation to the Suhongtu 1 Formation to be 37.6 °C/km, whereas that through the Bayingebi 2 Formation was found to be 27.4°C/km. This segmentation in the geothermal gradient is mainly attributed to differences in the thermal conductivities of the rock types in the different strata;

(3) The terrestrial heat flow in the Wuliji fault-nose tectonic zone of the Chagan sag is between 61.0 and 81.0 W/m^2, with an average value of 70.9 W/m^2. The terrestrial heat flow in the central tectonic belt is between 65.1 and 69.1 W/m^2, with an average value of 67.5 W/m^2. The terrestrial heat flow in the Chagan sag overall is 70.6 mW/m^2. These results imply that the geothermal state of the Chagan sag is between between tectonically stable and active areas.

Acknowledgements

This work was funded by the National Natural Science Foundation of China (grant no. 41374089, 41402219), the Foundation of the Geoscience Young Science Foundation of Liu Baojun (Grant No. DMSM2017003), the Sichuan Science & Technology Foundation (Grant No. 2016JQ0043), and the State Key Laboratory of Petroleum Resources and Prospecting, China University of Petroleum, Beijing (Grant No. PRP/open-1705). Our heartfelt gratitude also goes to Prof. Huang Shaopeng, Prof. Hu Shengbiao, Dr. Duan Wentao, Dr. Hu Di, M.S Wang Yi, M.S Fu Rao for their helpful suggestions of the manuscript.

Manuscript received Apr. 13, 2018
Accepted May 31, 2018
Associate EIC in charge: Hao Ziguo
Edited by Fei Hongcai

References

Carson, C.J., Mclaren, S., Roberts, J.L., Boger, S.D., and Blankenship, D.D., 2014. Hot rocks in a cold place: High sub–glacial heat flow in East Antarctica. *Journal of the Geological Society*, 171(1): 9–12.

Čermák, V., Balling, N., Kukkonen, I., and Zui, V.I., 1993. Heat flow in the baltic shield—results of the lithospheric geothermal modelling. *Precambrian Research*, 64(s1–4): 53–65.

Chang Jian, Qiu Nansheng, Zhao Xianzheng, Xu Wei, Xu Qiuchen, Jin Fengming, Han Chunyuan, Ma Xuefeng and Liang Xiaojuan, 2016. Present-day geothermal regime of the Jizhong depression in Bohai Bay basin, East China. *Chinese Journal of Geophysics*, 59(3): 1003–1016 (in Chinese with English abstract).

Chapman, D.S., 1984. Heat flow in the Uinta Basin determined from bottom hole temperature (BHT) data. *Geophysics*, 49(4): 453–466.

Che Zicheng, Liu Liang, Liu Hongfu and Luo Jinhai, 1998. The constituents of the Altun fault system and genetic characteristics of related Meso–Cenozoic petroleum–bearing basin. *Geological Bulletin of China*, 17(4): 377–384 (in Chinese with English abstract).

Chen Aihua, Xu Xing, Lou Xianhu, Liao Kaixun and Peng Deng, 2017. Heat flow characteristics and controlling factors of the Baikang basin in South China sea. *Acta Geologica Sinica*, 91(8): 1720–1728 (in Chinese with English abstract).

Chen Qilin, Wei Pingsheng and Yang Zhanlong, 2006. Tectonic evolution and petroleum prospection in the Yin'gen-Ejina basin. *Petroleum Geology and Experiment*, 28(4): 311–315 (in Chinese with English abstract).

Chen Changchun, 1994. A personal view on rotation drift movement of the Siberia plate. *World Regional Studies*, (1):

67–71 (in Chinese).
Chen Zhipeng, Ren Zhanli, Yu Chunyong, Qi Kai, Ren Wenbo, Yang Yan and Ma Qian, 2018. Characteristics and genetic analysis of hydrothermal sediment of Lower Cretaceous in Hari depression, Yin′e Basin. *Earth Science*, 43(6): 1941–1956 (in Chinese with English abstract).
Duchkov, A.D., Rychkova, K.M., Lebedev, V.I., Kamenskii, I.L., and Sokolova, L.S., 2010. Estimation of heat flow in Tuva from data on helium isotopes in thermal mineral springs. Russian *Geology & Geophysics*, 51(2): 209–219.
Feng Changge, Liu Shaowen, Wang Liangshu and Li Cheng, 2009. Present–day geothermal regime in Tarim basin, northwest China. *Chinese Journal of Geophysics*, 52(11): 2752–2762 (in Chinese with English abstract).
Furlong, K.P., and Chapman, D.S, 1987. Thermal state of the lithosphere. Reviews of Geophysics, 25(6): 1255–1264.
Gong Yuling, Wang Liangshu, Liu Shaowen, Li Cheng, Han Yongbing, Liu Bo and Cai Jingong, 2003. Terrestrial heat flow distribution in Jiyang depression in Bohai Bay basin, East China. *Science in China (Series D)*, 33(4): 384–391 (in Chinese).
Group Investigating Geothermic, Institute of Geology, Academia Sinica, 1979. The first portion of data of terrestrial heat flow measurements in China. *Acta Seismologica Sinica*, 1(1): 93–109 (in Chinese with English abstract).
Hao Chunyan, Liu Shaowen, Wang Huayu and Wang Liangshu, 2014. Global heat flow: An overview over past 20 years. *Chinese Journal of Geology*, 49(3), 754–770 (in Chinese with English abstract).
Hasterok, D., Chapman, D.S., and Davis, E.E., 2011. Oceanic heat flow: Implications for global heat loss. *Earth & Planetary Science Letters*, 311(3): 386–395.
He Lijuan, Xiong Liangping and Wang Jiyang, 1998. The geothermal characteristics in south China sea. *China Offshore Oil and Gas* (Geology), 13(2): 87–90 (in Chinese with English abstract).
Jiang Guangzheng, Gao Peng, Rao Song, Zhang Linyou, Tang Xiaoyin, Huang Fang, Zhao Ping, Tang Zhonghe, He Lijuan and Hu Shengbiao, 2016. Compilation of heat flow data in the continental area of China (4th edition). *Chinese Journal of Geophysics*, 59(8): 2892–2910 (in Chinese with English abstract).
Kukkonen, I.T., Rath, V., Kivekäs, L., Šafanda, J., and Čermak, V., 2011. Geothermal studies of the Outokumpu Deep Drill Hole, Finland: Vertical variation in heat flow and palaeoclimatic implications. *Physics of the Earth & Planetary Interiors*, 188(1–2): 9–25.
Leszek C., and Konrad J K., 2012. Thermal convection in the porous methane–soaked regolith in Titan: Finite amplitude convection. *Icarus*, 217(1): 130–143.
Li Zongxing, Gao Jun, Zheng Ce, Liu Chenglin, Ma Yinsheng and Zhao Weiyong, 2015. Present–day heat flow and tectonic thermal evolution since the late Paleozoic time of the Qaidam basin. *Chinese Journal of Geophysics*, 58(10): 3687–3705 (in Chinese with English abstract).
Liu Shaowen, Lei Xiao and Wang Liangshu, 2015. New heat flow determination in northern Tarim Craton, northwest China. *Geophysical Journal International*, 200(2): 1196–1206.
Liu Qianqian, Shi Yanan, Wei Dongping, Han Peng, Chen Shunyun, Liu Peixun and Liu Liqiang, 2017. Near-surface geothermal gradient observation and geothermal analyses in the Xianshuihe fault zone, eastern Tibetan plateau. *Acta Geologica Sinica*(English Edition), 91(2):414-428.
Liu Xi, Han Wei, Wei Jianshe and Zhang Yunpeng, 2017. Constraints of apatite fission track on the Mesozoic tectonic activities in Xirehada region, Yin'e Basin, Inner Mongolia. *Acta Geologica Sinica*, 91(10):2185-2195 (in Chinese with English abstract).
Lu Qingzhi, Hu Shengbiao, Guo Tonglou and Li Zhongping, 2005. The background of the geothermal field for formation of abnormal high pressure in the northeastern Sichuan basin. *Chinese Journal of Geophysics*, 48(5): 1110–1116 (in Chinese with English abstract).
Lysak, S.V., 1987. Terrestrial heat flow of continental rifts. *Tectonophysics*, 143(1–3): 31–41.
Meng Lingshun, Guan Ye, Qi Li and Gao Rui, 1995. Gravity field and deep crustal structure in Golmud–Ejin Qi geoscience transection and nearby area. *Chinese Journal of Geophysics*, 38(S2): 36–45 (in Chinese with English abstract).
Morgan, P., 1982. *Heat flow in rift zones*. American Geophysical Union, 107–122.
Peng Heng, Wang Jianqiang, Massimiliano Zattin, Liu Chiyang, Han Peng and Zhang Shaohua, 2018. Late Triassic-Early Jurassic uplifting in eastern Qilian Mountain and its geological significance: Evidence from apatite fission track thermochronology. *Earth Science*, 43(6): 1983–1996 (in Chinese with English abstract).
Pollack, H.N., Hurter, S.J., and Johnson, J.R, 1993. Heat flow from the earth's interior: analysis of the global data set. *Reviews of Geophysics*, 31(3): 267–280.
Qiu Nansheng, 1998. Thermal status profile in terrestrial sedimentary basins in China. *Advances in Earth Sciences*, 13(5): 447–451 (in Chinese with English abstract).
Qiu Nansheng, 2001. Research on heat flow and temperature distribution of the Qaidam basin. *Journal of China University of Mining & Technology*, 30(4): 412–415 (in Chinese with English abstract).
Qiu Nansheng, 2002. Characters of thermal conductivity and radiogenic heat production rate in basins of northwest China. *Chinese Journal of Geology*, 37(2): 196–206 (in Chinese with English abstract).
Qiu Nansheng, 2003. Geothermal regime in the Qaidam basin, northeast Qinghai Tibet Plateau. *Geological Magazine*, 140(6): 707–719.
Ranalli ? and Rybach ?, 2005. Heat flow, heat transfer and lithosphere rheology in geothermal areas: Features and examples. *Journal of Volcanology & Geothermal Research*, 148(1): 3–19.
Rao Song, Hu Shengbiao, Zhu Chuanqing, Tang Xiaoyin, Li Weiwei and Wang Jiyang, 2013. The characteristics of heat flow and lithospheric thermal structure in Junggar basin, northwest China. *Chinese Journal of Geophysics*, 56(8): 2760–2770 (in Chinese with English abstract).
Rudnick, R.L., Mcdonough, W.F., and O'Connell, R.J., 1998. Thermal structure, thickness and composition of

continental lithosphere. *Chemical Geology*, 145(3–4): 395–411.
Ruepke, L., Schmid, D., and Souche, A., 2017. Interrelation between surface and basement heat flow in sedimentary basins. *AAPG Bulletin*, 101(10): 1697–1713.
Wang Chunyan, Lin Changsong, Wu Maobing, Gong Gu and Zheng Menglin, 2006. Tectonic evolution and petroleum prospects of the Mesozoic Inggen-Ejin Qi basin, Inner Mongolia. *Geology in China*, 33(6): 1328–1335 (in Chinese with English abstract).
Wang Xinwen, Tao Guoqiang, 2008. Structural framework and evolution of Chagan sag in Inner Mongolia. *Geoscience*, 22(04): 495–504 (in Chinese with English abstract).
Wang Liangshu, Liu Shaowen, Xiao Weiyong, Li Cheng, Guo Suiping, Liu Bo, Luo Yuhui and Cai Dongsheng, 2002. The heat flow characteristic in Bohai Bay basin. *Chinese Science Bulletin*, 47(2): 151–155 (in Chinese).
Wang Shenglang, Shi Peng, Zhang Fangdong and Qi Renli, 2016. Petroleum geologic features and exploration discovery in Chagan sag. *China Petroleum Exploration*, 21(3): 108–115 (in Chinese with English abstract).
Wang Tianyang, Li Guobiao, Li Xinfa and Niu Xiaolu, 2017. Early eocene radiolarian fauna from the sangdanlin, southern tibet: constraints on the timing of initial India-Asia collision. *Acta Geologica Sinica*(English Edition), 91(6): 1964–1977.
Wang Yongxin and Feng Diansheng, 2003. Present–day geothermal field and thermal history of eastern subdepression, Liaohe basin. *Chinese Journal of Geophysics*, 46(2): 197–202 (in Chinese with English abstract).
Wei Pingsheng, Zhang Huquan, Lin Weidong and Li Anchun, 2005. Exploration prospects for oil and gas in Yinggen–Ejinaqi basin. *Natural Gas Industry*, 25(3): 7–10 (in Chinese).
Wu Tairan and He Guoqi, 1993. Tectonic units and their fundamental characteristics on the northern margin of the Alxa block. *Acta Geologica Sinica*, 67(2): 97–108 (in Chinese with English abstract).
Xu Ming, Zhu Chuanqing, Tian Yuntao, Rao Song and Hu Shengbiao, 2011. Borehole temperature logging and characteristics of subsurface temperature in the Sichuan basin. *Chinese Journal of Geophysics*, 54(4): 1052–1060 (in Chinese with English abstract).
Xu Zhiqin, Yang Jingsui, Zhang Jianxin, Jiang Mei, Li Haibing and Cui Junwen, 1999. A comparison between the tectonic units on the two sides of the Altun sinistral strike-slip fault and the mechanism of lithospheric shearing. *Acta Geologica Sinica*, 73(3): 193–205 (in Chinese with English abstract).
Xu Zhiqin, Yang Jingsui, Li Haibing, Ji Shaocheng, Zhang Zeming and Liu Yan, 2011. On the tectonics of the India–Asia collision. *Acta Geologica Sinica*, 85(1): 1–33 (in Chinese with English abstract).
Yang Jinlin, 2011. Discussion on intraland plate moving evolvement in China and the relationship with earthquake. *Inland Earthquake*, 25(2): 109–119 (in Chinese with English abstract).
Yi Shanfeng, 1966. Introduction to the world geothermal survey case. *Geology Express*, (4): 10–13 (in Chinese).
Zhou Yang, Mu Genxu, Zhang Hui, Wang Ke, Liu Jianqiang and Zhang Yage, 2017. Geothermal field division and its geological influencing factors in Guanzhong basin. *Geology in China*, 44(5): 1017–1026 (in Chinese with English abstract).
Zuo Yinhui, Qiu Nansheng, Zhang Yuan, Li Cuicui, Li Jinping, Guo Yonghua and Pang Xiongqi, 2011. Geothermal regime and hydrocarbon kitchen evolution of the offshore Bohai Bay basin, North China. *AAPG Bulletin*, 95(5): 749–769.
Zuo Yinhui, Qiu Nansheng, Deng Yixun, Rao Song, Xu Shenmou and Li Jianguo, 2013a. Terrestrial heat flow in the Qagan sag, Inner Mongolia. *Chinese Journal of Geophysics*, 56(9): 3038–3050 (in Chinese with English abstract).
Zuo Yinhui, Ma Weimin, Deng Jixun, Hao Qingqing, Li Xinjun, Guo Junmei, Ran Qing and Wang Lirong, 2013b. Mesozoic and Cenozoic thermal history and source rock thermal evolution history in the Chagan sag, Inner Mongolia. Editorial *Committee of Earth Science–Journal of China University of Geosciences*, 38(3): 553–560 (in Chinese with English abstract).
Zuo Yinhui, Qiu Nansheng, Hao Qingqing, Zhang Yunxian, Pang Xiongqi, Li Zhongchao and Gao Xia, 2014. Present geothermal fields of the Dongpu sag in the Bohai Bay Basin. *Acta Geologica Sinica* (English Edition), 88(3): 915–930.
Zuo Yinhui, Qiu Nansheng, Hao Qingqing, Pang Xiongqi, Gao Xia, Wang Xuejun, Luo Xiaoping and Zhao Zhongying, 2015a. Geothermal regime and source rock thermal evolution history in the Chagan sag, Inner Mongolia. *Marine and petroleum Geology*, 59: 245–267.
Zuo Yinhui, Zhang Wang, Li Zhaoying, Li Jiawei, Hao Qingqing and Hu Jie, 2015b. Mesozic and Cenozoic tectono thermal evolution history in the Chagan sag, Inner Mongolia. *Chinese Journal of Geophysics*, 58(7): 2366–2379 (in Chinese with English abstract).
Zuo Yinhui, Ye Bin, Wu Wenting, Zhang Yunxian, Ma Wenxin, Tang Shilin and Zhou Yongshui, 2017a. Present temperature field and Cenozoic thermal history in the Dongpu depression, Bohai Bay Basin, North China. *Marine and Petroleum Geology*, 88: 696–711.
Zuo Yinhui, Song Rongcai, Li Zongxing Wang Yixuan and Yang Meihua, 2017b. Lower Cretaceous source rock evaluation and thermal maturity evolution of the Chagan depression, Inner Mongolia, Northern China. E*nergy Exploration & Exploitation*, 35(7):1–22.

About the first author:

FENG Renpeng, male; born in 1993 in Xuanhan County, Sichuan Province; Master candidate of Mineral Resource Prospecting and Exploration, Chengdu University of Technology. He is now interested in the study on the present geothermal fields and tectono-thermal history of the sedimentary basin. E-mail: fengrpeng@163.com;

phone:13540222725.

About the corresponding author:

ZUO Yinhui, male; born in 1980 in Deyang city, Sichuan Province; Doctor; associate professor of State Key Laboratory of Oil and Gas Geology and Exploitation, Chengdu University of Technology. He is now interested in the study on the present geothermal fields and tectono-thermal history of the sedimentary basin and hydrocarbon accumulation history analysis. E-mail: zuoyinhui@tom.com; phone:18280398276.